

Jon C. Gottschalck*¹, Paul R. Houser¹, and Xubin Zeng²¹ NASA / GSFC – UMBC / GEST, Greenbelt, Maryland² University of Arizona, Tucson, Arizona

1. INTRODUCTION

The parameterization of vegetation in land surface models plays a major role in the simulation of the surface energy balance and therefore weather and climate prediction. Historically, parameters in land surface process models have been assigned based on generalized land surface classifications that do not account for local anomalies in phenology. More recently, however, there have been studies that have incorporated satellite remote sensing data in the parameterization of the vegetation used in land surface models (Sellers et al. 1996; Los et al. 2000; Zeng et al. 2001). Satellite data provides better spatial and temporal resolution and so improved sampling of the seasonal variability of critical vegetation parameters such as leaf area index (LAI) and fractional vegetation cover. Our hypothesis is that using these improved remotely-sensed parameters may produce improved land surface simulations and our group is actively working on incorporating satellite remote sensing data into the Global Land Data Assimilation System (GLDAS, <http://ldas.gsfc.nasa.gov>) currently being developed at NASA's Goddard Space Flight Center and at NOAA's National Center for Environmental Prediction. This paper presents the current state of this work -- our initial methodology and preliminary findings.

2. METHODOLOGY

In this paper we evaluate the changes in LAI via the Community Land Model Version 2 (CLM2). Our original version of CLM2 assigns LAI according to a limited set of classes (1 km University of Maryland (UMD) vegetation classification), each of which designates a maximum and minimum value of LAI (Table 1). The LAI at any given time varies seasonally between these two values depending on deep layer soil temperature. This assignment of LAI is

used in the first GLDAS simulation. The second uses LAI data from Boston University (<http://cybele.bu.edu>) developed from the Advanced Very High Resolution Radiometer (AVHRR).

Type	ENeed	EBroad	DNeed	DBroad
Max	6.00	6.00	6.00	6.00
Min	5.00	5.00	1.00	1.00
Type	MixedF	Woods	W/Grass	CShrub
Max	6.00	6.00	5.13	6.00
Min	3.00	3.49	2.08	2.00
Type	OShrub	Grass	Crops	Urban
Max	6.00	2.00	6.00	5.00
Min	1.00	0.50	0.96	1.00

Table 1: Maximum and minimum LAI for the UMD vegetation classification. Values apply for evergreen needleleaf trees, evergreen broadleaf trees, deciduous needleleaf trees, deciduous broadleaf trees, mixed forest, woodlands, mixed woodlands / grassland / shrubland, closed shrubland, open shrubland, grassland, cropland, and urban areas.

The LAI data was derived from values of normalized difference vegetation index (NDVI) in combination with a radiative transfer model for a number of vegetation types and has a spatial resolution of 8 km (Myeni et al. 1997). The monthly data used in this study is a climatology from the years 1981-1992. Preliminary validation of the satellite LAI dataset are promising (Buerman et al. 2001). In the near future we plan to use non-climatological monthly data and also begin to incorporate 1 km data from the Moderate resolution Imaging Spectroradiometer (MODIS).

It is important to highlight at this time the improvements in the satellite dataset. First, the AVHRR derived dataset provides improved spatial and temporal sampling. Second, although the original LAI designation does provide some sense of the seasonality of the vegetation due to the dependence on deep soil layer temperature, they apply *globally* for a given vegetation type. On the other hand, both latitudinal and longitudinal variations are accounted for in the satellite data. Third, anomalies in LAI due to varying weather

* Corresponding author address: Jon C. Gottschalck, Hydrological Sciences Branch – Code 974, NASA / Goddard Space Flight Center, Greenbelt, MD 20771; e-mail: jgotts@hsb.gsfc.nasa.gov.

regimes (*i.e.*, drought) and agricultural schedules are included as a function of the geographical region.

In order to attempt to represent the variability in each 8 km pixel as a function of vegetation type, a 1 km LAI dataset was constructed by using three items: (1) the 8 km LAI data, (2) the 1 km UMD vegetation type classification, and (3) mean 8 km LAI data that is defined as a function of 10° latitude zone, month of year, and vegetation type. This mean value quantifies how the LAI data of different vegetation types relate to each other as a function of month and latitude zone (Zeng, X. et al. 2001). Therefore, the 1 km LAI values vary both higher and lower than the 8 km LAI based on this mean but also are impacted by the percentage of each of the vegetation types in the 8 km pixel (in order to provide some information to weight the predominant vegetation types). The above relationships are constrained to the 8 km LAI value. Moreover, each 1 km LAI value was divided by a 1 km fractional vegetation cover in order to obtain a 1 km LAI value for vegetated area only. Table 2 shows an example of this procedure for a 8 km pixel that contains three vegetation types.

Conditions: 8 km LAI=5.0, July, 40° N, 50% evergreen needleleaf trees (V1), 25% cropland (V2), 25% open shrubland (V3)
Means for July, 40°N: V1 = 4.9, V2 = 2.5, V3 = 0.9
$V1=(4.9/4.9) * V1, V2=(2.5/4.9) * V1, V3=(0.9/4.9) * V1$
$32/64 * V1 + 16/64 * V2 + 16/64 * V3 = 5.0$
Solving for V1 (evergreen trees) LAI = 7.4, similarly for V2 (cropland) LAI = 4.3, V3 (open shrubland) LAI = 1.4

Table 2: The procedure for constructing the 1 km LAI dataset from the 8 km AVHRR LAI dataset. The first row shows the conditions (location and 8 km pixel attributes) for this example. The second and third rows indicate the means that apply for 40° N for July for each vegetation type and how they relate to each other. The fourth row illustrates the relationship used to constrain the outcome to the 8 km LAI value and to weight the respective vegetation types. The final row indicates the 1 km LAI value for the vegetation types in that 8 km pixel.

Once the 1 km LAI data is estimated, the 1 km LAI values for the predominant vegetation type in each 0.25° grid box were averaged and these values were input into GLDAS via CLM2. Figure 1 illustrates for June 2001 the respective LAI fields for both of the LAI designations at 0.25°. Large sections of the eastern United States, the boreal forests in Canada and Asia, the Amazon, and sections of central Africa show similar magnitudes in LAI with parts of the Mississippi Valley,

southeast US, and central Plains being notable exceptions. However, there are some large global differences. Much lower LAI values are the norm across many areas of the globe such as the western US, Mexico, east-central South America, central and southern Africa, Australia, and sections of Europe and southeast Asia.

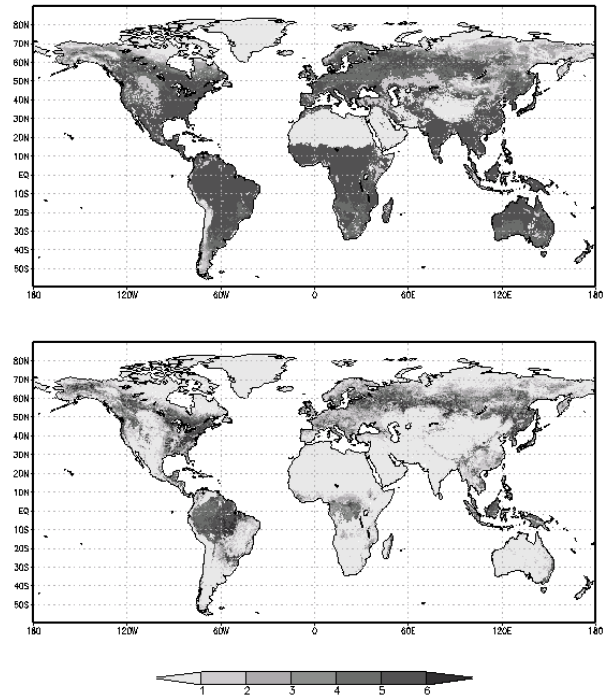


Figure 1: LAI assigned based on a given maximum LAI, minimum LAI, and deep layer soil temperature (top) and LAI derived from AVHRR (bottom). Both panels apply for June 2001.

The preliminary results presented here comprise a month long simulation for June 2001 for the two assignments of LAI. The model runs were initialized and forced with meteorology data from the National Center for Environmental Prediction (NCEP) Global Data Assimilation System (GDAS). The GLDAS simulations were conducted at 0.25 x 0.25 resolution at hourly time-steps.

3. RESULTS AND DISCUSSION

Differences in the assignment of LAI impact a number of processes and variables in CLM2. In this paper we focus on canopy transpiration, soil surface temperature, and total column soil moisture and focus on North America for the sake of clarity. Figure 2 illustrates the difference in canopy transpiration (original LAI – AVHRR LAI)

between the two model simulations after one month. There are some substantial differences mainly over the central and western areas of North America (transpiration lower with the AVHRR LAI) caused by the assignment of much higher values of LAI in the original CLM2 (Figure 1). The vegetation types in these areas include grassland and shrubland that equate to lower LAI values using the radiative transfer algorithm than what other datasets have shown (Sellers et al. 1996; Los et al. 2000). In addition, large areas of cropland in this region are impacted by weather and agricultural changes. The absolute magnitudes in canopy transpiration for the model runs ranged up to 350 Wm^{-2} .

Less canopy transpiration alters the surface energy balance through lower total latent heat flux. Figure 3 illustrates the difference in soil surface temperature and shows a signature very similar to that of Figure 2 with warmer soil surface

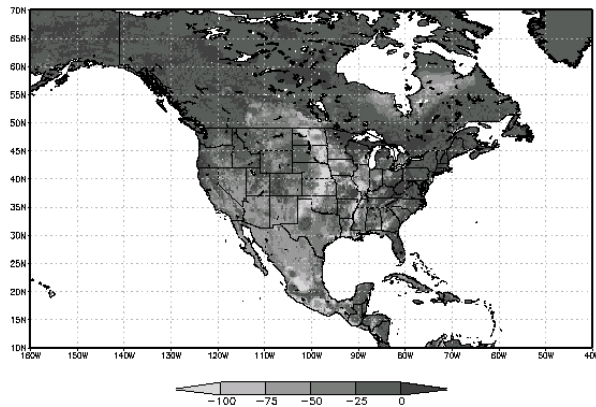


Figure 2: Difference in canopy transpiration (original LAI – AVHRR LAI) in Wm^{-2} valid on 30 June 2001.

temperatures in western North America and in parts of the southeast US and Mississippi River valley where the AVHRR dataset indicates areas of lower LAI. In addition, greater solar radiation enters the soil and allows higher temperatures. The differences are substantial and are range up to and over 10° C warmer for the AVHRR simulation in parts of the central and western US and Mexico. The AVHRR simulation also shows that the soil surface temperature across the whole continent for the most part is warmer than with the original LAI designation. The absolute temperatures in both model runs generally ranged from $260 - 330 \text{ }^\circ\text{K}$ globally.

The lower transpiration in these areas limits the loss of total soil moisture content for the AVHRR simulation (Figure 4). The soil is significantly moister across Mexico for instance.

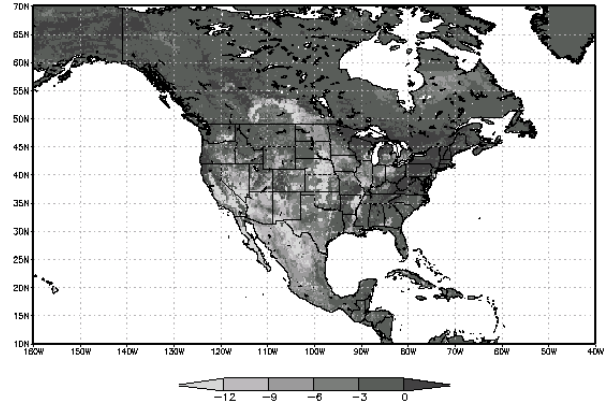


Figure 3: Difference in soil surface temperature (original LAI – AVHRR LAI) in $^\circ\text{K}$ valid on 30 June 2001.

Other areas across the globe also show this impact such as in east-central South America (not shown). The impact of these issues will only intensify as the seasonal time scale is reached and may have large impacts on local surface temperature and climate on interannual time scales.

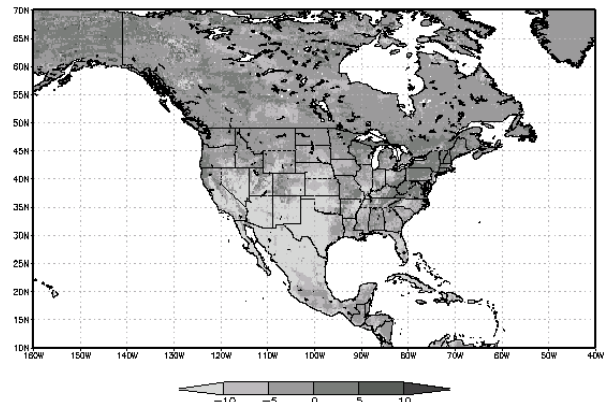


Figure 4: Difference in total column soil moisture content (original LAI – AVHRR LAI) in mm valid on 30 June 2001.

Our hypothesis is that the AVHRR LAI dataset will highlight local anomalies in phenology due to weather and land use variations and improve the simulation. Our group plans to evaluate our simulations by comparing our model output to satellite derived surface temperature from the Geostationary Operational Environmental Satellite (GOES) and MODIS as well as other in-situ data sources. We also plan on integrating over a seasonal time period with additional observed forcing datasets.

4. REFERENCES

Buermann, W., J. Dong, X. Zeng, R. Myneni, R. E. Dickinson, 2001: Evaluation of the utility of satellite-based vegetation leaf area index data for climate simulations. Submitted to *Journal of Climate*.

Los, S. O., G. J. Collatz, P. J. Sellers, C. M. Malmstrom, N. H. Pollack, R. S. Defries, L. Bounoua, M. T. Parris, C. J. Tucker, and D. A. Dazlich, 2000: A global 9-yr biophysical land surface dataset from NOAA AVHRR Data. *Journal of Hydrometeorology*, 1, 183-199.

Myneni, R. B., R. R. Nemani, and S. W. Running, 1997: Algorithm for the estimation of global land cover, LAI and FPAR based on radiative transfer

models. *IEEE Trans. Geosc. Remote Sens.*, 35: 1380-1393.

Sellers, P. J., S. O. Los, C. J. Tucker, C. O. Justice, D. A. Dazlich, G. J. Collatz, and D. A. Randall, 1996: A revised land surface parameterization (SiB2) for atmospheric GCMs. Part II: The generation of global fields of terrestrial biophysical parameters from satellite data. *Journal of Climate*, 9, 706-737.

Zeng, X., R. E. Dickinson, A. Walker, M. Shaikh, R. S. Defries, and J. Qi, 2000: Derivation and evaluation of global 1-km fractional vegetation cover data for land modeling. *J. Appl. Met.*, 39, 826-839.

Zeng, X., M. Shaikh, Y. Dai, R. E. Dickinson, and R. Myneni, 2001: Coupling of the Common Land Model to the NCAR Community Climate Model. Submitted to *Journal of Climate*.